TÜBİTAK

Turkish Journal of Physics

http://journals.tubitak.gov.tr/physics/

Research Article

Turk J Phys
(2018) 42: 478 – 483

doi:10.3906/fiz-1805-2

Forward-backward asymmetry of Drell–Yan lepton pairs at 14 TeV center-of-mass energy

Kamuran DİLSİZ[1,*], **Hasan OĞUL**[2]

[1]Department of Physics, Faculty of Arts and Sciences, Bingöl University, Bingöl, Turkey

[2]Department of Nuclear Engineering, Faculty of Engineering and Architecture, Sinop University, Sinop, Turkey

Received: 04.05.2018 • **Accepted/Published Online:** 24.07.2018 • **Final Version:** 15.08.2018

Abstract: In this paper, fiducial cross-sections of lepton pairs with opposite charge via $Z \rightarrow l^+l^-$ ($l^{\pm} = \mu^{\pm}, e^{\pm}$) are calculated at a center-of-mass energy of 14 TeV by applying different transverse momentum selections to evaluate their impact on the production cross-section as well as the differential cross-section of Z bosons in terms of lepton pseudorapidity. The predictions are computed by next-to-next-to-leading order quantum chromodynamics including next-to-leading order electroweak corrections. Forward-backward asymmetry prediction for the Drell–Yan production in proton-proton collision is further calculated at 14 TeV using HERAPDF2.0, MMHT2014, NNPDF3.1, and CT14 parton distribution function models. Then 14 TeV QCD predictions of forward-backward asymmetry are presented as a function of dilepton mass for four different Z boson rapidity regions.

Key words: Forward-backward asymmetry, differential cross-sections, hadron-hadron scattering

1. Introduction

The Large Hadron Collider (LHC) [1] is the most powerful proton-proton (pp) collider in the world. At the LHC, there are two general-purpose detectors called CMS [2] and ATLAS [3], which have different geometries to record the events coming from pp interactions. The first proton beam was circulated at the LHC with a center-of-mass energy of 7 TeV in 2010 [1]. The higher center-of-mass energy increases the probability of finding new particles and allows checking the accuracy of the predictions that are theoretically available. Therefore, the center-of-mass energy at the LHC was increased to 8 TeV in 2012 and 13 TeV in 2015. In the current accelerator facility at the LHC, there will be an upgrade starting in 2019 and the center-of-mass energy will be increased to 14 TeV.

The most complete theory that explains elementary particles and the interactions between them is the standard model (SM). The long missing piece of the SM was the Higgs boson, which was observed by the ATLAS and CMS collaborations at the LHC [4,5]. The measurements on the Higgs boson have so far been compatible with the predictions from the SM, but precision measurements are still needed to confirm that there are no deviations from these predictions, pointing to new physics. The weak interactions via W and Z bosons are the main backgrounds in the Higgs boson measurements. In this regard, we have previously reported the QCD cross-section predictions of inclusive Z bosons at $\sqrt{s} = 14$ TeV [6].

The differential QCD predictions and measurements of the Drell–Yan process are crucial since the Drell–Yan process provides a major source of background for measurements with top quark, ZZ resonances, and high

*Correspondence: kdilsiz@bingol.edu.tr

mass dilepton resonances [7]. Since the Drell–Yan process includes both vector and axial-vector couplings of electroweak bosons to fermions, the process also involves a forward-backward asymmetry (A_{FB}) originating from these vector and axial-vector couplings [8]. CMS and ATLAS collaborations have previously reported the A_{FB} measurements of lepton pairs with opposite charges produced by the reaction $pp \rightarrow Z/\gamma^* \rightarrow l^+l^-$, where l refers to an electron or a muon [8,9].

In this article, we present theoretical predictions of Drell–Yan production by using the FEWZ 3.1 Monte Carlo (MC) program [10]. In order to obtain A_{FB} predictions, differential QCD predictions of the Drell–Yan process were computed as a function of dilepton mass and presented in four different absolute rapidity (y) regions.

2. Methodology

All predictions in this analysis were performed by using the FEWZ 3.1 program that is the commonly used MC program for Z boson studies. In this section, we present fiducial cross-sections with different lepton p_T thresholds. As shown in Figure 1, the p_T regions were selected as (>0, 25, 35, 55). Then the predictions are repeated 50 times in each p_T region to suppress statistical fluctuation; therefore, the values are fitted with a straight line to find the average value of extracted numbers. The fitted average values are assigned as the predicted values. This method is applied all predictions presented in this paper, including A_{FB} calculations.

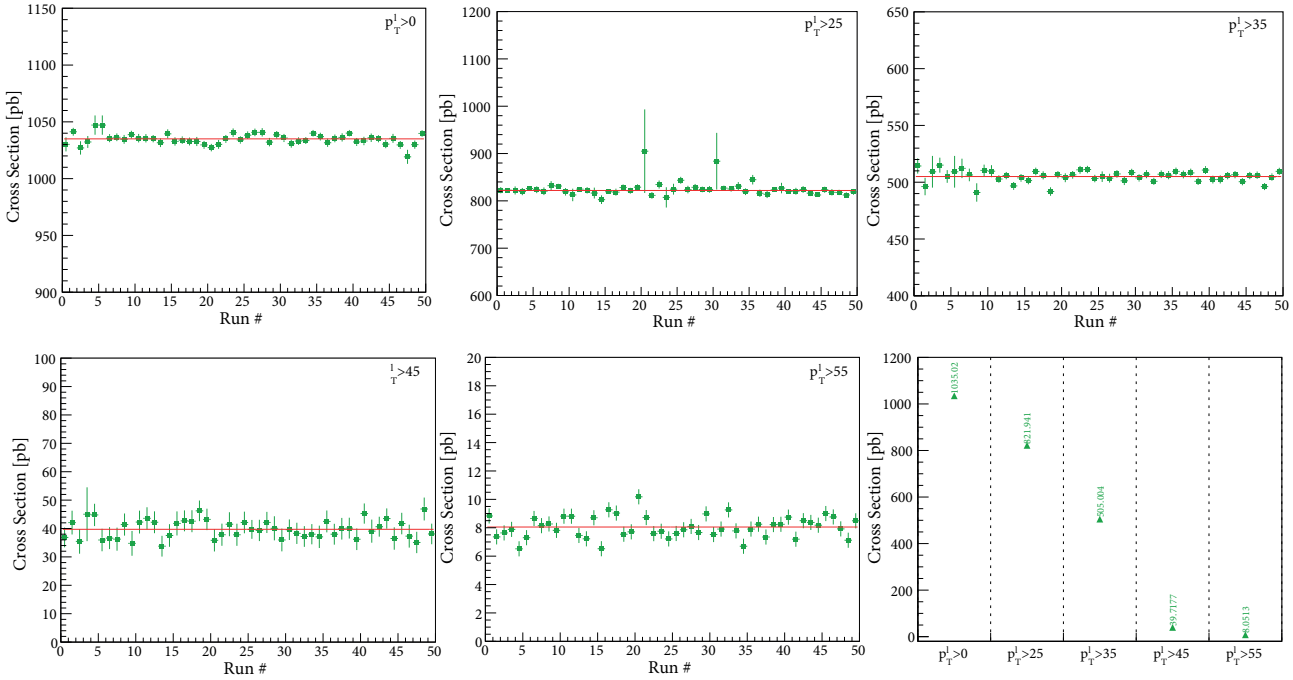

Figure 1. Method for the extraction of QCD predictions in different transverse momentum regions.

3. Cross-section and differential cross-section

QCD predictions of elementary particles are useful to estimate the value of the cross-section of a particle in the future experimental runs that will operate at higher energies. QCD predictions of Z bosons are theoretically available at leading order (LO), next-to-leading order (NLO), and next-to-next-to-leading order (NNLO). With the increased center-of-mass energy at the LHC, higher order predictions of the cross-section become important

for better modeling of the expected data. We therefore perform NNLO QCD predictions of the cross-section in $pp \to Z \to l^+l^-$ interaction at $\sqrt{s} = 14$ TeV. These results will be useful for the experimentalists at CERN for the next LHC run.

Figure 2 shows the differential cross-section of $pp \to Z \to l^+l^-$ as a function of lepton pseudorapidity ($|\eta|$) at $\sqrt{s} = 14$ TeV. Five different thresholds are used on the p_T of leptons and the applied p_T cuts on both charged leptons are required to be the same. As can be seen, the differential cross-section decreases when the required threshold on the p_T is increased. Similarly, the differential cross-section decreases when $|\eta|$ is increased.

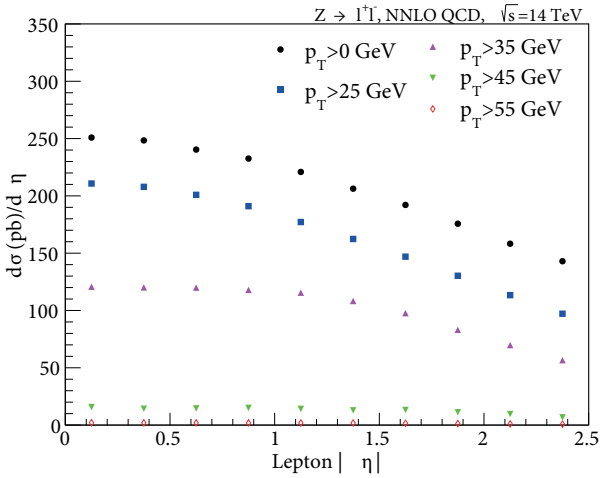

Figure 2. Differential cross-section of $Z \to l^+l^-$ decay at NNLO QCD. The predictions are performed at $\sqrt{s} = 14$ TeV.

4. Forward-backward asymmetry

Forward-backward asymmetry of Drell–Yan production is caused by vector and axial vector couplings of quark-antiquark annihilation in pp collisions. The cross-section for the annihilation process is given by Eq. (1):

$$\frac{d(\sigma)}{d(cos\theta)} = \frac{4\pi\alpha^2}{3\hat{s}}\left[\frac{3}{8}A\left(1 + cos^2\theta\right) + Bcos\theta\right], \tag{1}$$

where α is the fine structure constant, $\sqrt{\hat{s}}$ is the center-of-mass energy of quark and antiquark pairs, and θ is the angle between the charged lepton and the quark that is in the rest frame of the dileptons. A and B are coefficients that are functions of $\sqrt{\hat{s}}$ and vector and axial vector couplings. To minimize the impact of nonvanishing p_T, a particular rest frame of the dilepton system that is called the Collins–Soper (CS) frame [11] is selected. In this way, the angle between the lepton and quark can be calculated by Eq. (2):

$$\cos\theta_{cs} = \frac{p_{z,ll}}{|p_{z,ll}|}\frac{2(p_1^+p_2^- - p_1^-p_2^+)}{m_{ll},\sqrt{m_{ll}^2 + p_{T,ll}^2}} \text{ and } p_i^{\pm} = \frac{1}{\sqrt{2}}(E_i \pm p_{z,i}), \tag{2}$$

where p_z is the longitudinal momentum for the (anti) lepton $(i = 2)\, i = 1$, E is the energy, and m_{ll} is the invariant mass of the dilepton system. Using this $\cos\theta$, we calculate A_{FB} as shown in Eq. (3) by selecting

$\cos\theta > 0$ for the forward (σ_F) and $\cos\theta < 0$ for the backward (σ_B) events:

$$A_{FB} = \frac{\sigma_F - \sigma_B}{\sigma_F + \sigma_B}. \tag{3}$$

The reliability of the FEWZ 3.1 program has been already studied at 7, 8, and 13 TeV, and the agreement between the predicted and observed results was found to be remarkable [6,12]. Therefore, we assume that the program will also be valid at 14 TeV. However, we use HERAPDF2.0 as the reference parton distribution function (PDF) model and the other PDF predictions are used to be cross-checked.

We report forward-backward asymmetry results for the Z boson as a function of dilepton mass at four different rapidity regions in the Table. A_{FB} predictions are obtained by using the HERAPDF2.0 PDF model at NNLO QCD. These predictions are presented in 14 different dilepton mass windows to be consistent with the latest A_{FB} paper [8].

Table. A_{FB} predictions at 14 TeV using HERAPDF2.0 PDF model at NNLO QCD.

A_{FB} predictions at 14 TeV				
$M_{l^+l^-}$ bin	$0 < \|y\|$	$1.0 < \|y\| < 1.25$	$1.25 < \|y\| < 1.50$	$1.50 < \|y\| < 2.40$
40–50	0.0195	0.0317	0.0027	0.0262
50–60	–0.0108	0.0060	–0.0363	–0.0055
60–76	–0.0287	–0.0485	–0.1045	–0.0895
76–86	–0.0047	–0.0139	–0.0086	–0.0458
86–96	0.0087	0.0186	0.0251	0.0238
96–106	0.0236	0.0587	0.0727	0.0818
106–120	0.0449	0.1166	0.0010	0.1248
120–133	0.0543	0.1487	0.1502	0.1791
133–150	0.0131	0.1643	0.1646	0.2129
150–171	0.0836	0.1794	0.1527	0.1921
171–200	0.0937	0.1696	0.2423	0.2344
200–320	0.1075	0.2452	0.2679	0.2435
320–500	0.1529	0.3283	0.3389	0.2900
500–2000	0.1746	0.1489	0.0660	0.4291

Figure 3 shows a comparison of $\cos\theta$ distributions for different center-of-mass energies, PDFs, and rapidity regions. On the left-hand side plot in Figure 3, $\cos\theta$ distributions are compared at different center-of-mass energies of 8, 13, and 14 TeV, which are roughly consistent. The middle plot in Figure 3 shows a comparison of $\cos\theta$ distributions obtained by HERAPDF2.0, MMHT2014, NNPDF3.1, and CT14 PDF sets, which are in good agreement. Finally, the right-hand side plot in Figure 3 compares the $\cos\theta$ distributions in four different rapidity regions. This explains why we could have very different A_{FB} results in different regions.

5. Results and discussion

This study presents NNLO QCD predictions of two oppositely charged lepton pairs emerging from pp interaction at $\sqrt{s} = 14$ TeV to provide A_{FB} predictions for the next LHC run. We first investigate the impact of the different transverse momentum selections, which are applied to leptons in physics analyses. In order to suppress

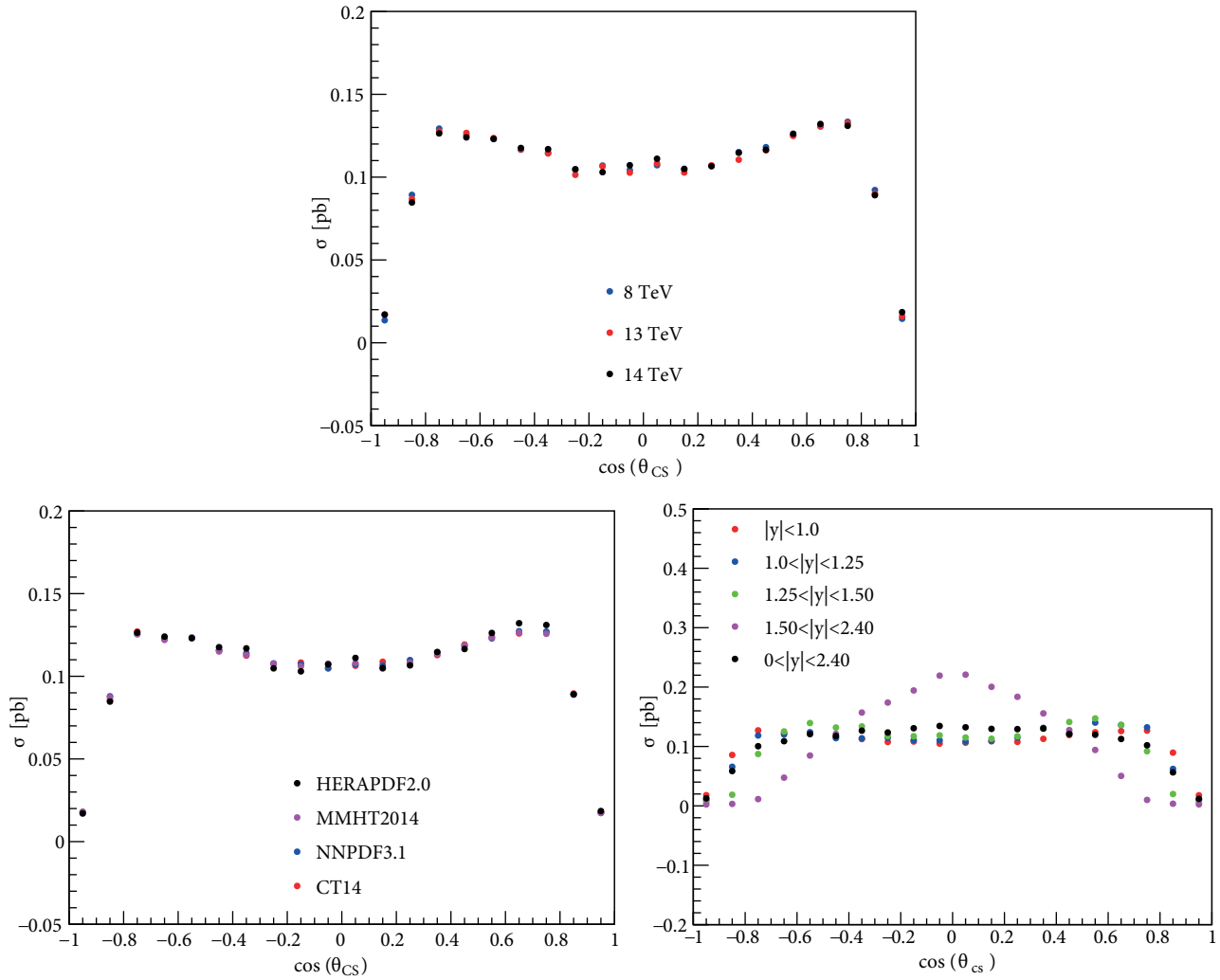

Figure 3. $\cos\theta$ distributions at different energy levels (top), comparison of different PDF models at $\sqrt{s} = 14$ TeV (bottom left), and comparison of $\cos\theta$ distributions in different rapidity regions (bottom right).

any false claim or judgment, a method that performs production and differential cross-sections of Z bosons is developed. The results show that the cross-section decreases with increasing lepton p_T or |eta|.

A_{FB} at $\sqrt{s} = 14$ TeV is calculated by using a publicly available MC tool, FEWZ 3.1. The consistency of FEWZ 3.1, which was interfaced with the HERAPDF2.0 PDF model, was previously confirmed by comparing the QCD predictions of W and Z bosons with publicly available experimental results [6,12]. In this study, we present A_{FB} results that are obtained by using the HERAPDF2.0 PDF model at $\sqrt{s} = 14$ TeV. The results are obtained for 14 different dilepton mass ranges and four different rapidity regions, as given in the Table. As can be seen in the Table, A_{FB} shows differences at different dilepton masses and rapidity regions.

$\cos\theta$ distributions that provide the angle between a lepton and a quark are also calculated for various center-of-mass energies, PDFs, and rapidity regions. The results show that the distributions of cross-sections as a function of $\cos\theta$ at center-of-mass energies of 8, 13, and 14 TeV are consistent with each other. A similar level of agreement is also obtained for $\cos\theta$ distributions with four different PDF models (HERAPDF2.0, MMHT2014,

NNPDF3.1, CT14) at a center-of-mass energy of 14 TeV. However, $\cos\theta$ distribution results that are obtained at four different rapidity regions (0–1, 1–1.25, 1.25–1.50, 1.50–2.40) show differences from each other.

Acknowledgment

This work was supported by the Sinop University Scientific Research Projects Coordination Unit, Project Number MMF-1901-17-08, 2017.

References

[1] Evans, L.; Bryant, P. *J. Instrum.* **2008**, *3*, S08001.

[2] Bayatian, G. L.; Chatrchyan, S.; Sirunyan, A. M.; Adam, W.; Bergauer, T.; Dragicevic, M.; Erö, J.; Friedl, M.; Fruehwirth, R.; Ghete, V. et al. *CMS-TDR-008-1*; CERN: Geneva, Switzerland, 2006.

[3] Aad, G.; Bentevelsen, S.; Bobbink, G. J.; Bos, K.; Boterenbrood, H.; Brouwer, G.; Buis, E. J.; Buskop, J. J. F.; Colijn, A. P.; Dankers, R. et al. *J. Instrum.* **2008**, *3*, S08003.

[4] Aad, G.; Abajyan, T.; Abbott, B.; Abdallah, J.; Khalek, S. A.; Abdelalim, A. A.; Abdinov, O.; Aben, R.; Abi, B.; Abolins, M. et al. *Phys. Lett. B* **2012**, *716*, 1-29.

[5] Chatrchyan, S.; Khachatryan, V.; Sirunyan, A. M.; Tumasyan, A.; Adam, W.; Bergauer, T.; Dragicevic, M.; Erö, J.; Fabjan, C.; Friedl, M. et al. *Nat. Phys.* **2014**, *10*, 557-560.

[6] Ogul, H.; Dilsiz, K. *Adv. High Energy Phys.* **2017**, *2017*, 8262018.

[7] Chatrchyan, S.; Khachatryan, V.; Sirunyan, A. M.; Tumasyan, A.; Adam, W.; Bergauer, T.; Dragicevic, M.; Erö, J.; Fabjan, C.; Friedl, M. et al. *J. High Energy Phys.* **2011**, *10*, 1-41.

[8] Khachatryan, V.; Sirunyan, A. M.; Tumasyan, A.; Adam, W.; Asilar, E.; Bergauer, T.; Brandstetter, J.; Brondolin, E.; Dragicevic, M.; Erö, J. et al. *Eur. Phys. J. C* **2016**, *76*, 325.

[9] Aad, G.; Abbott, B.; Abdallah, J.; Khalek, S. A.; Abdelalim, A. A.; Abdinov, O.; Aben, R.; Abi, B.; Abolins, M.; AbouZeid, O. S. et al. *J. High Energy Phys.* **2015**, *9*, 1-42.

[10] Li, Y.; Petriello, F. *Phys. Rev. D* **2012**, *86*, 094034.

[11] Collins, J. C.; Soper, D. E. *Phys. Rev. D* **1977**, *16*, 2219.

[12] Ogul, H.; Dilsiz, K.; Tiras, E.; Tan, P.; Onel, Y.; Nachtman, J. *Adv. High Energy Phys.* **2016**, *2016*, 7865689.